Development of Neutron Resonance Transmission Analysis as a Non-Destructive Assay Technique for Nuclear Nonproliferation*)

Harufumi TSUCHIYA, Fumito KITATANI, Makoto MAEDA, Yosuke TOH and Masatoshi KURETA

Nuclear Science and Engineering Center, Japan Atomic Energy Agency, 2-4 Tokai-mura, Naka-gun, Ibaraki 319-1195, Japan

(Received 8 June 2017 / Accepted 22 October 2017)

Currently, there is much demand for a non-destructive assay technique to quantify special nuclear materials of ^{235}U and Pu isotopes in a field of nuclear nonproliferation. For this purpose, a compact NRTA system is under development. The performance of a proposed compact NRTA system was investigated by calculating a neutron transmission spectrum for a spent nuclear fuel. In this paper, we mainly evaluated how a transmission spectrum was affected by neutron pulse width and flight path length of the system and discuss the appropriate values from a viewpoint of measurement of special nuclear materials.

Keywords: special nuclear material, neutron resonance transmission analysis

DOI: 10.1585/pfr.13.2406004

1. Introduction

From a viewpoint of nuclear nonproliferation, it is very important to evaluate the amount of special nuclear materials (SNMs; ^{235}U and Pu isotopes) and minor actinides (MAs) in nuclear fuels such as a spent fuel, fuel debris and a next generation fuel for transmutation. These quantifications require an accurate and short-time measurement, even though those fuels have too high dose rates for us to treat them easily. Thus, a non-destructive assay (NDA) technique has been considered as a promising one.

A passive neutron NDA technique measures neutrons that are derived from spontaneous fissions of SNMs. It would be difficult to conduct such measurements since the targets themselves contain a lot of other spontaneously fissionable materials (e.g. ^{244}Cm) and fission fragments that emit vast amounts of neutrons and gamma rays. The same is true of a passive gamma-ray NDA method. Unlike a passive NDA method, an active NDA one uses an external source as a diagnostic tool. For example, the differential die-way analysis (DDA) [1] or the delayed neutron (DN) technique [2] uses a 14 MeV neutron generator (DT tube) to induce fissions of fissile materials (^{235}U, ^{239,241}Pu). If such an external source is intense enough to overcome high radiations from the fuels, it will be able to determine the amount of fissile materials, but, it is, in principle, difficult to directly evaluate the amount of fertile ones.

Neutron Resonance Transmission Analysis (NRTA) is one of active NDA techniques. It is based on a time-of-flight (TOF) technique that relies on a well-established principle. Behrens *et al.* [3] actually determined the amount of SNMs and some MAs in a cut spent fuel, with an accuracy of 1 - 20%. This clearly shows a sufficient potential of NRTA to quantify fissile and fertile materials in nuclear fuels. However, their measurements were accomplished by a large NRTA system with an electron linear accelerator that produces intense neutron beams with a short pulse width (250 ns). It is impossible to apply such a large NRTA system to an existing facility such as a reprocessing one. To solve the problem, we started developing a compact NRTA system specially designed for quantifications of SNMs in nuclear fuels.

2. Compact NRTA System

2.1 Basic of NRTA

The basic principle of NRTA is well described in [4]. Thus, we briefly explain it from a viewpoint of practical usage.

Figure 1 shows total cross sections of uranium and plutonium. As clearly shown, SNMs have one or more strong resonances in the energy region. Importantly each resonance appears at a specific energy. By measuring the specific energy with a TOF method, NRTA makes use of such resonances as nucleus fingerprints to distinguish individual resonances.

NRTA needs pulsed neutron beams to evaluate the neutron energy E_n with the TOF method. A TOF t_{tof} is experimentally computed from the time difference between a stop time (t_d) and a start time (t_0). Here t_d and t_0 are given by a neutron detector and a neutron generator, respectively. The t_{tof} is related to the E_n by a simple formula of

author's e-mail: tsuchiya.harufumi@jaea.go.jp

*) This article is based on the presentation at the Conference on Laser Energy Science / Laser and Accelerator Neutron Sources and Applications 2017.

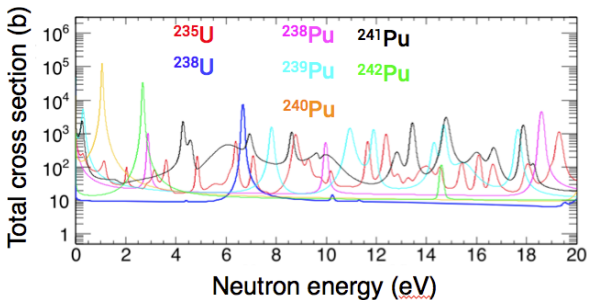

Fig. 1 Total cross sections of U and Pu in energy range 0 - 20 eV. The data are obtained from JENDL-4.0 [5].

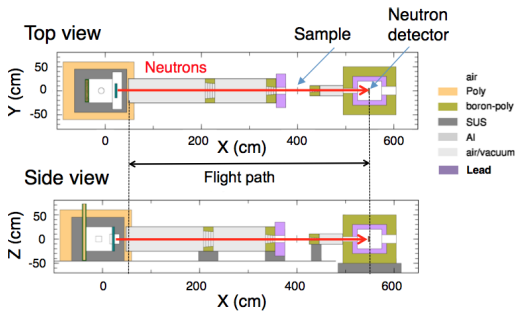

Fig. 2 Schematic view of a compact NRTA system with a flight path length of 5 m.

$$E_{\mathrm{n}} = \frac{1}{2} m \left(\frac{L}{t_{\mathrm{tof}}} \right)^2 , \tag{1}$$

where m is the neutron rest mass and L represents a flight path length or a distance from a neutron source to a neutron detector. This formula is valid for the non-relativistic energy region.

The quantity of interest for NRTA is the probability that a neutron passes a sample without any interaction, which is called the transmission T. To obtain this T, a neutron beam is irradiated to a sample. Some of them are transmitted through it with no interaction, measured by a neutron detector. The T is deduced from a ratio of counts of sample-in measurement C_{in} and sample-out one C_{out}. Here the sample-in (sample-out) measurement shows a measurement with (without) the sample. An experimental transmittion T_{exp} is defined as

$$T_{\mathrm{exp}} = \frac{C_{\mathrm{in}}}{C_{\mathrm{out}}}. \tag{2}$$

Under an ideal experiment, T is shown by

$$T = \exp\left(- \sum_{\mathrm{k}} n_{\mathrm{k}} \cdot \sigma_k(E_{\mathrm{n}}) \right), \tag{3}$$

where n_{k} and σ_{k} are the areal number density and the total cross section of nuclide k, respectively. One can obtain σ_{k} and the corresponding resonance parameters from the major evaluated nuclear data libraries such as JENDL [5]. Thus, we can deduce n_{k} by analyzing T_{exp} with σ_{k}

2.2 Energy resolution of NRTA

From Eq. (1), an energy resolution $\Delta E_{\mathrm{n}}/E_{\mathrm{n}}$ can be derived as a following equation,

$$\frac{\Delta E_{\mathrm{n}}}{E_{\mathrm{n}}} = 2 \sqrt{ \left(\frac{\Delta L}{L} \right)^2 + \left(\frac{\Delta t}{t_{\mathrm{tof}}} \right)^2 }. \tag{4}$$

In the right term, ΔL and Δt represent uncertainties of L and t_{tof}, respectively. Generally, it is easy to measure L with a small ΔL (e.g. 1 mm or less for L of a few m or longer), and hence the term related to L can be small practically. As discussed in [4], the Δt depends on several factors including a pulse width of a neutron generator. As the pulse width is shorter, the Δt becomes smaller; a shorter pulse width makes $\Delta E_{\mathrm{n}}/E_{\mathrm{n}}$ better. Similarly, a larger L and the resultant larger t_{tof} also results in a better energy resolution, but an intense neutron source would be required for practical measurement so as to compensate a small neutron flux at a distant position. Thus, to make a compact NRTA system, we must consider a flight path length and a pulse width of neutron beams.

2.3 Concept of a compact NRTA system

A compact NRTA system requires a compact neutron source that produces pulsed neutron beams to determine the neutron energy. According to [6], a commercial DT tube can offer pulsed neutron beams with neutron yield of $\sim 10^8$ - 10^{10} n/s with its pulse width of 10 µs. Its size of at most a meter length and a ~10 cm diameter also matches our requirement. Although a DT tube has been mainly applied to DN instruments and DDA ones [6] until now, we consider a DT tube as one candidate of a neutron generator in a compact NRTA system.

A current NRTA facility uses a large-size and sophisticated accelerator to yield neutrons with $\sim 10^{12}$ - 10^{15} n/s [7, 8]. Their pulse width, ranging from a few nano seconds to ~1 µs, is rather shorter than a DT tube. In addition to such a large accelerator, a small-size X–band electron linac or a proton one is being developed as a compact neutron source for several applications [7, 8]. These small-size accelerators have a pulse width of ~1 µs or longer. At present, an electron linac is more compact than a proton one. Thus, as another candidate of a neutron source, we consider a small electron linac with a pulse width of 1 µs.

In addition to the above candidates, there are other neutron sources utilizing a laser [9] or inertial electrostatic confinement [10]. However they does not give appropriate pulsed neutrons for NRTA measurement at present. Therefore, we considered the above two possibilities.

Our concept of development of a compact NRTA system is that it is packed in a container such as a 40-feet type one (length ~12 m). Figure 2 shows its schematic design consisting of 3 parts: a neutron source, a flight path tube and a detector (left to right in Fig. 2). Emitted from the source part, generated neutrons have relatively high

energy. Those neutrons are reflected and moderated by stainless steel (SUS) and polyethylenes, with their energies reduced to the epithermal region that is suitable for SNM measurements. The produced neutrons are delivered through a flight path tube and irradiated to a sample. Collimators, consisting of borated polyethylenes and leads, are installed in the flight path to prevent scattered neutrons and/or gamma rays from reaching a sample and a neutron detector. The transmitted neutrons are detected by a neutron detector such as a ^{6}Li-glass scintillation one. The detector is surrounded by leads and borated polyethylene.

3. Results

3.1 Energy spectrum

In order to quantify SNMs in a low energy region of 0.1 - 20 eV, it is important for the neutron source to enhance neutron flux in the energy region. Because high-energy neutrons produced are efficiently moderated by hydrogen in polyethylenes, we investigated with MCNP simulations how polyethylenes at an entrance of the flight path affects neutron flux. Figure 3 shows derived neutron energy spectra at the entrance (top). For comparison, those at a detector position (bottom) are drawn as well. All the neutron spectra have a similar form with a peak at around 0.05 eV and above the peak energy they are generally expressed by a power-law function. As shown, the derived neutron spectrum with 3 cm polyethylene gives higher fluxes in the relevant energy region than the other ones. This trend remains the same in the neutron spectrum at a detector position.

For check, Table 1 lists neutron fluences that are integrated over several energy regions at an entrance of the flight path. It is found that the derived neutron fluence in 0.1 - 20 eV for thickness of 3 cm is higher than the other flueneces for 1 cm and 5 cm by a factor of 1.25 and 1.48, respectively. The reason would be that a 3 cm thickness polyethylenes is suitable to efficiently moderate neutrons and release them.

3.2 Application to a spent fuel

To understand how well a compact NRTA system measures SNMs in a spent fuel, we calculated a transmission spectrum expected for a spent fuel with a burn-up ratio of 30 GWd/t by adopting the neutron spectrum obtained for 3-cm polyethylene (Fig. 3). Here, weight percent ratios of U and Pu in a 30 GWd/t spent fuel were taken from [11]. A sample thickness is assumed to be 1 cm. In this work, we focus on impacts of a pulse width and a flight path length on a transmission spectrum.

Figure 4 shows two transmission spectra assuming a pulse width of 10 μs (black) and 1 μs (red). The two spectra below 2 eV have little difference in shape, both indicating the presence of ^{239,240,242}Pu. It is very important for a compact NRTA system to detect signatures of ^{240,242}Pu that are not fissile, because a DDA technique and a DN one, that have been used for measurement of nuclear materials,

Table 1 Neutron fluences (cm^{-2})* at an entrance of the flight path.

Thickness (cm)	0.01 - 0.1 eV	0.1 - 20 eV	20 - 100 eV
	($\times 10^{-5}$)	($\times 10^{-5}$)	($\times 10^{-5}$)
1	5.7	3.2	1.6
3	8.7	4.0	1.4
5	7.5	2.7	0.8

* Statistical errors for individual fluences are smaller than 1×10^{-8}.

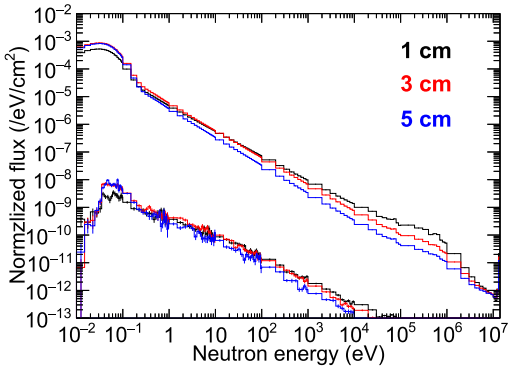

Fig. 3 Neutron energy spectra at an entrance of the flight path (top) and a detector position (bottom). The vertical axis denotes normalized flux that is divided by the total number of simulated neutrons. Colors correspond to thicknesses of polyethylenes at an entrance of the flight path. Quoted errors are statistical 1σ.

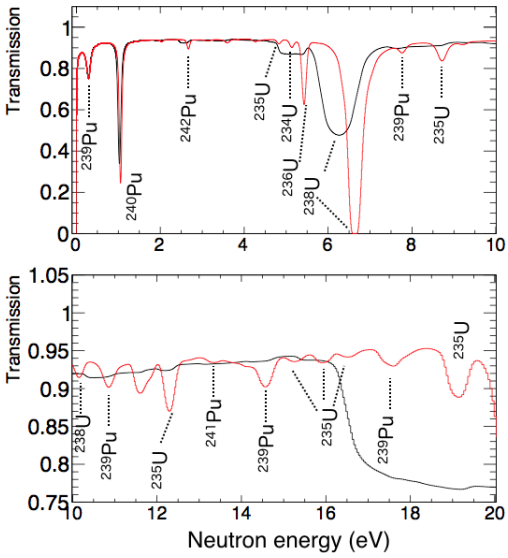

Fig. 4 Comparison of transmission spectra assuming a pulse width is 10 μs (black) or 1 μs (red). The flight path length is fixed at 5 m. Top and bottom panels show transmission in 0 - 10 eV and 10 - 20 eV, respectively.

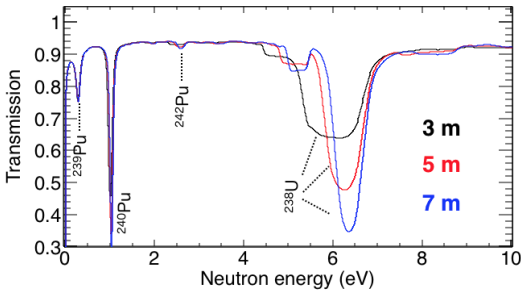

Fig. 5 Comparison of transmission spectra assuming a flight path length is 3 m (black), 5 m (red) and 7 m (blue). A pulse width is 10 μs. An energy range is 0 - 10 eV.

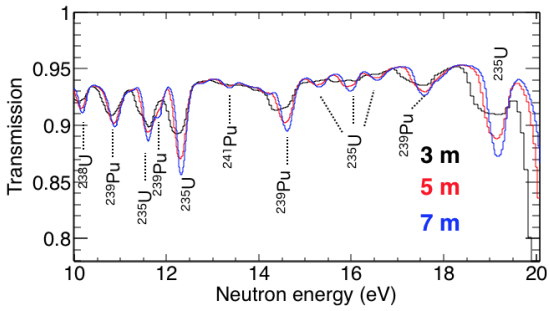

Fig. 6 The same as Fig. 5, but a pulse width is 1 μs. An energy range is 10 - 20 eV.

are basically sensitive only to fissile materials, not to these fertile ones [2]. The difference between the two spectra becomes remarkable in the higher energy region. Compared with the transmission spectrum for 1 μs, that for 10 μs has no clear resonance dips at >10 eV (bottom panel of Fig. 4). Consequently, it is found that the 10 μ transmission spectrum can identify ^{238}U and ^{239,240,242}Pu and the 1 μ one not only them but also ^{235}U and ^{241}Pu. This difference in detection of SNMs between the two spectra is attributable to variations of energy resolution according to Eq. (4). As a remark, this drawback of a compact NRTA system with the 10 μs pulse width can be compensated when it is incorporated with the DDA system as suggested by [1].

Figure 5 shows three transmission spectra calculated under a flight path length of 3, 5 and 7 m. Because a compact NRTA system is assumed to be in a 40-feet container, the 7 m length will be the maximum when we take account of size of the other parts as well as space for working. The 3-m transmission spectrum cannot well resolve a resonance dip of ^{242}Pu at 2.6 eV due to poor energy resolution of ~15% calculated by Eq. (4) assuming Δt = 10 μs. The L term in Eq. (4) was neglected because it is sufficiently small compared to the t one as mentioned in Sec. 2.2. In addition, the ^{238}U resonance dip at 6.67 eV in the 3-m transmission is considerably broader compared with that for transmission of 5 m or 7 m. This difference shows that the 6.67-eV resonance shape for each transmission strongly depends on each energy resolution of ~24% (3 m), ~14% (5 m) and ~10% (7 m).

A transmission spectrum under a pulse width of 1 μs was also computed with a flight path length changed. As a result, three transmission spectra at <10 eV were found to be almost the same as one another. On the other hand, from Fig. 6 we found that a flight-path length affected the transmission spectra in 10 - 20 eV. Compared with the transmission spectrum for 3 m, those for 5 m and 7 m give clearer resonance dips. In addition, a resonance dip of ^{241}Pu at 13.4 eV was unable to be found in the 3-m spectrum while seen in the other two spectra. Given these results, we may conclude that a flight path length of 5 m - 7 m is appropriate for a compact NRTA system with pulse widths of 1 - 10 μs.

4. Summary

The performances of a compact NRTA system were investigated with its neutron pulse width and flight path length changed. First a transmission spectrum for a 30 GWd/t spent fuel was calculated with a flight path length fixed at 5 m, assuming a neutron pulse width of 1 μs or 10 μs. The former pulse width gives better energy resolution, allowing us to identify SNMs with many resonance dips. Then, by changing a flight path length to 3 m, 5 m or 7 m, we found that a 5 m - 7 m flight path would be suitable for the SNM measurement with a compact NRTA system with its pulse width of 1 - 10 μs.

Acknowledgments

This work was partly done under the agreement between JAEA and EURATOM in the field of nuclear materials safeguards research and development. This work is supported by MEXT.

[1] M. Kureta *et al.*, Proc. the 57th INMM annual meeting (2016).
[2] P. Blanc *et al.*, LA-UA **10-04125** (2010).
[3] J.W. Behrens *et al.*, Nucl. Tech. **67**, 162 (1984).
[4] P. Schillebeeckx *et al.*, Nucl. Data Sheets **113**, 3054 (2012).
[5] K. Shibata *et al.*, Nucl. Sci. Tech. **48**, 1 (2011).
[6] B.A. Ludewigt, LBNL-**4426** (2011).
[7] M. Uesaka and H. Kobayashi, Rev. Accel. Sci. Tech. **8**, 181 (2015).
[8] I.S. Anderson *et al.*, Phys. Rep. **654**, 1 (2016).
[9] Y. Arikawa *et al.*, Plasma Fusion Res. **10**, 2404003 (2015).
[10] K. Masuda *et al.* in "Nuclear physics and Gamma-ray sources for nuclear security and nonproleferation", edited by T. Hayakawa, M. Senzaki and others (World Scientific), 195 (2015).
[11] H. Uetsuka *et al.*, JAERI-Rep. **95-084** (1995) [in Japanese].